

Supporting Information

for

Strong and fast-recovery Organic/inorganic hybrid AuNPs-Supramolecular gels based on Loofah-like 3D networks

Huiwen He^{as}, Si Chen^{as*}, Xiaoqian Tong^a, Yining Chen^a, Bozhen Wu^a, Meng Ma^a, Xiaosong Wang^b and Xu Wang^{a*}

^a College of Materials Science and Engineering, Zhejiang University of Technology, Hangzhou 310014, China. Phone: 86-0571-88320855, Fax: 86-0571-88320855.

^b xiaosong.wang@uwaterloo.ca

*Email: wangxu@zjut.edu.cn, sichen@zjut.edu.cn.

1 Synthesis and characterization of the gelators and AuNPs

1.1 Materials

All materials employed in the paper were commercial available. Octa (3-aminopropyl) silsesquioxanes hydrochloride (Octa-Ammonium POSS-HCl) was purchased from hybrid plastic (Hattiesburg, MS). N,N,N,N'-Tetram-ethyl-O-(1H-benzotriazol-1-yl)uroniumhexafluorophosphate (HBTU), 1-hydroxybenzotriazole(HOBt), BOC-L-Homophenylalanine, Boc-Cys(Bzl)-OH, tetraoctylammonium bromide (TOABr), chloroauric acid (HAuCl₄), Sodium borohydride (NaBH₄), and N-Methylmorpholine (NMM) were supplied by Aladdin(Shanghai, China), and used as received. 1-hexadecylthiol (HDT) was supplied by Alfa Aesar (American). All solvents used in the synthesis were analytical pure and used without further purification. Silica column chromatography was carried out using silica gel (200-300 mesh) provided by Qingdao Haiyang Chemical (Qingdao, China). Thin layer chromatography was performed on commercially available glass backed silica plates.

1.2 Synthesis and characterization of POSS-Cys

The structure and synthetic route of POSS-Cys were presented on **Scheme S1**, the synthesis process was similar to the literature¹. 3.10 g (10 mmol) Boc-Cys(Bzl)-OH, 3.80 g (10 mmol)

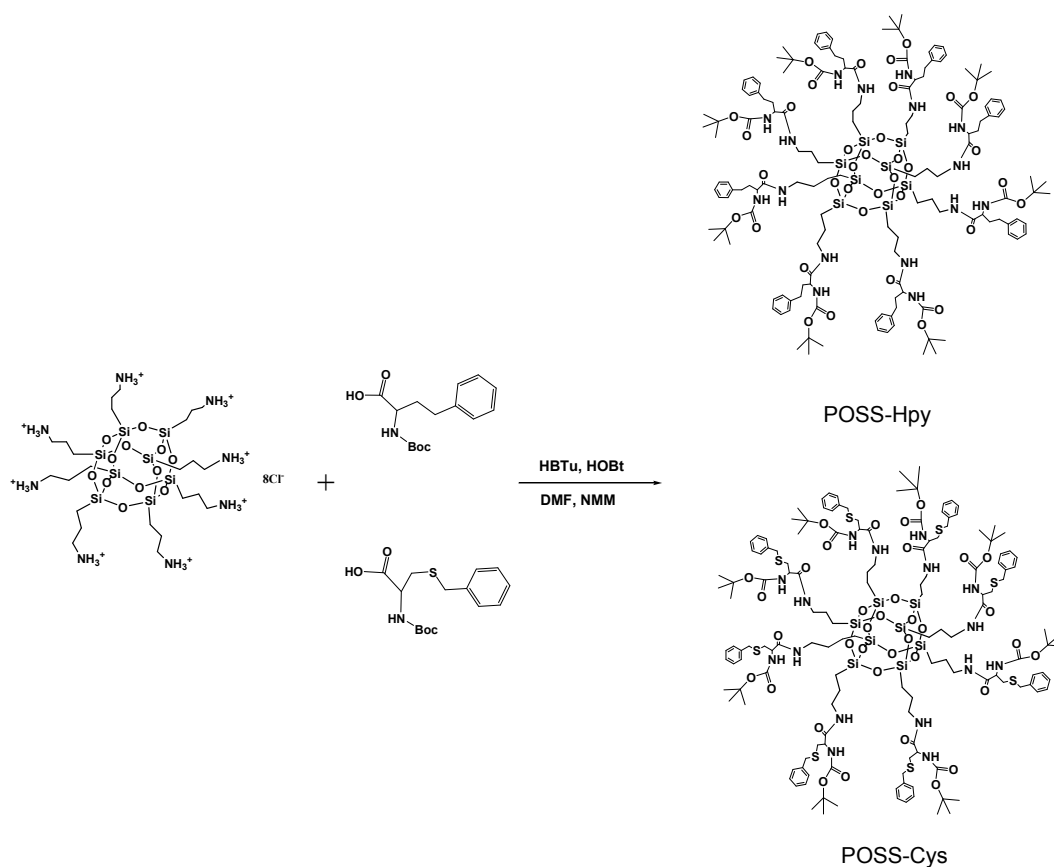
HBTU and 1.49 g (11 mmol) HOBt were dissolved in 20 mL DMF. After 5 min, 0.94 g (0.8 mmol) OctaAmmonium POSS-HCl and 1.66 g (16.4 mmol) NMM were added. The reaction mixture was stirred at room temperature for 24 h, and then 150 mL distilled water was added to get a white solid. The crude product was purified by column chromatography (silica, CH₂Cl₂: MeOH, 6:1) to get a white solid with the yield of 70%. The structure of the POSS-Cys was determined by NMR (Bruker Avance III, 500 MHz), ESI-TOF MS (Agilent 6210). **¹H NMR (DMSO-d₆, 500 MHz, ppm), δ** 8.04 (8H, br, CONH), 6.93 (8H, d, NHBoc), 7.21-7.32 (40H, m, Ar-H), 4.17 (8H, br, COCH(R)NH), 3.74 (16H, d, C₆H₅CH₂), 3.34 (16H, br, CH₂NH), 3.04 (16H, br, CHCH₂S), 1.46 (16H, br, SiCH₂CH₂), 1.37-1.40 (72H, m, CH₃), 0.57 (16H, br, SiCH₂); **¹³C NMR (CDCl₃, 125 MHz, ppm), δ**: 9.08, 23.00, 28.40, 34.15, 36.49, 41.95, 54.40, 80.00, 127.08, 128.52, 129.04, 138.03, 156.20, 171.25; **FTIR (KBr) ν** = 3280, 2930, 1650, 1530, 1450, 1360, 1240, 1110, 862, 771, 700, and 480 cm⁻¹; **ESI-TOF**: the calculated [M+H+Na]²⁺/2 of POSS-Cys was 1623.50 and the test result was 1623.60. The calculated [M+2H]²⁺/2 of POSS-Cys was 1614.50 and the test result was 1613.60, results fit with the calculation.

1.3 Synthesis and characterization of POSS-Hpy

The structure and synthetic route of POSS-Hpy were presented on **Scheme S1**, the synthesis process was similar to the synthesis of POSS-Cys. 1.40 g (5 mmol) BOC-L-Homophenylalanine, 1.90 g (5 mmol) HBTU and 0.75g (5.5 mmol) HOBt were dissolved in 20 mL DMF. After 5 min, 0.47 g (0.4 mmol) Octa-ammonium POSS-HCl and 0.83 g (8.2 mmol) NMM were added. The reaction mixture was stirred at room temperature for 24 h, and then 150 mL distilled water was added to get a white solid. The crude product was purified by column chromatography (silica, CH₂Cl₂: MeOH, 6:1) to get a white solid with the yield of 78%. **¹H NMR (CDCl₃, 500 MHz, ppm), δ**: 7.71 (8H, br, CONH), 6.07 (8H, d, NHBoc), 7.05-7.48 (40H, m, Ar-H), 4.31 (8H, br, COCH(R)NH), 3.32 (16H, br, CH₂NH), 3.06 (16H, d, C₆H₅CH₂), 2.74 (16H, br, CHCH₂), 1.97 (16H, br, SiCH₂CH₂), 1.27-1.64 (72H, m, CH₃), 0.6 (16H, br, SiCH₂). **¹³C NMR (CDCl₃, 125 MHz, ppm), δ**: 9.08, 22.84, 28.45, 32.20, 35.02, 41.87, 50.88, 79.63, 125.93, 128.33, 128.50, 141.38, 156.29, 172.80; **FTIR (KBr) ν** = 3310, 2930, 1660, 1530, 1450, 1370, 1240, 1110, 868, 754, 696, and 488 cm⁻¹; **ESI-TOF**: The calculated [M+2H]²⁺/2 of POSS-Hpy was 1490.70 and the test result was 1490.07. The calculated [M+H+Na]²⁺/2 of POSS-Hpy was 1505.20 and the test result was 1505.00, results fit with the calculation.

1.4 Synthesis of AuNPs

The AuNPs was synthesized according to the method published by Brust and co-workers². 30 mL (30 mM) HAuCl₄ aqueous solution was added in 80 mL (50 mM) TOABr toluene solution and stirred for 10 minutes. The two-phase mixture was vigorously stirred until all the HAuCl₄ was transferred into the organic layer and HDT (170 mg) was then added to the organic phase. 25 mL (0.4 M) freshly prepared aqueous solution of NaBH₄ was slowly added with vigorous stirring. After further stirring for 3h, the organic phase was separated, and evaporated to 10 mL in a rotary evaporator and mixed with 400 mL ethanol to remove excess thiol. The mixture was kept for 12 h at -18 °C and the dark brown precipitate was filtered off and washed with ethanol. The crude product was dissolved in 10 mL toluene and precipitated with 400 mL ethanol again. The final product was filtered off the precipitate after 6 h and dried at room temperature to get the AuNPs solid sol.



Scheme S1. The synthesis scheme for hybrid gelators POSS-Cys and POSS-Hpy

1.5 Fluorescence Spectroscopy

Fluorescence spectra of peptide gel samples were recorded on a Hitachi Spectrofluorimeter (model 650-40). The fluorescence spectrum of peptide gel samples was analyzed with pyrene as fluorescent probe. The fluorescence emission spectrum of pyrene, upon excitation at 335 nm, shows five vibronic peaks. The polarity of the interior of peptide gels was studied by comparing the relative intensity of peak I to peak III of pyrene monomer fluorescence.³

2. Additional Figures and Discussion

2.1 Characterization of AuNPs

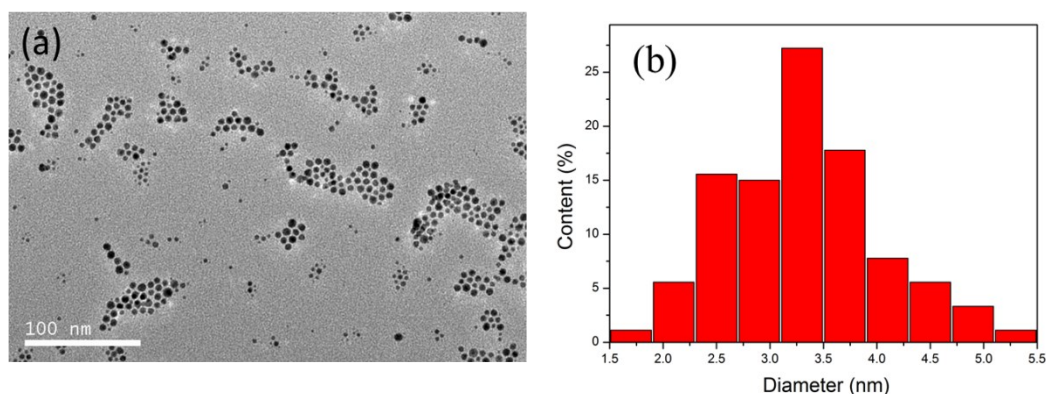


Figure S1. (a) TEM images of AuNPs, (b) AuNPs particle size distribution histograms.

2.2 Gelation ability and thermal stability

The gelation ability of novel hybrid gelators POSS-Cys and POSS-Hpy were examined in various organic solvents (Table S1). Kamlet-Taft model was used in order to better understand the effect of solvent on gelation⁴. It evidenced that gels were best supported in those solvents where α parameter is zero, β parameter is low meanwhile π^* parameter is high — i.e., toluene, benzene, chlorobenzene, styrene. The minimal gel concentration (MGC) of these gels were all below 20 mg/mL (2% w/v), indicative of high efficiency of gelating solvents for POSS-Cys and POSS-Hpy. What's more, most of these gels were highly transparent and thermally stable for a few months at room temperature (Figure S2).

Table S1. Gelation behaviour of POSS-Cys and POSS-Hpy in various solvents^a

Solvents	α	β	π^*	POSS-Cys	POSS-Hpy
<i>n</i> -hexane	0.00	0.00	-0.08	P	P
cyclohexane	0.00	0.00	0.00	P	P
toluene	0.00	0.11	0.54	TG (9.1)	TG(14.3)
benzene	0.00	0.10	0.59	TG (10.0)	TG(5.3)
chlorobenzene	0.00	0.07	0.71	TG (14.3)	TG(20.0)
xylene	0.00	0.03	0.80	P	TG(12.5)
styrene	0.00	N/A	N/A	TG(12.5)	TG(16.7)
methyl methacrylate	0.00	N/A	N/A	P	P
ethyl acetate	0.00	0.45	0.55	P	P
butyl acetate	0.00	N/A	0.46	P	P
acetone	0.08	0.48	0.71	P	OG(3.3)
THF	0.00	0.55	0.58	S	S
chloroform	0.44	0.00	0.69	S	S
dichloromethane	0.30	0.00	0.73	S	S
ethanol	0.83	0.77	0.54	P	S
methanol	0.93	0.62	0.60	S	S

^a P = precipitate, TG = transparent gel, OG = Opaque gel, VS = vicious solution, S = solution. α , β , π^* are the Kamlet-Taft parameters relating to the ability of the solvent to donate and accept hydrogen bonds and a generalized polarity parameter, respectively, N/A = not available. The data in brackets represents the minimal gel concentration (MGC), mg/mL.

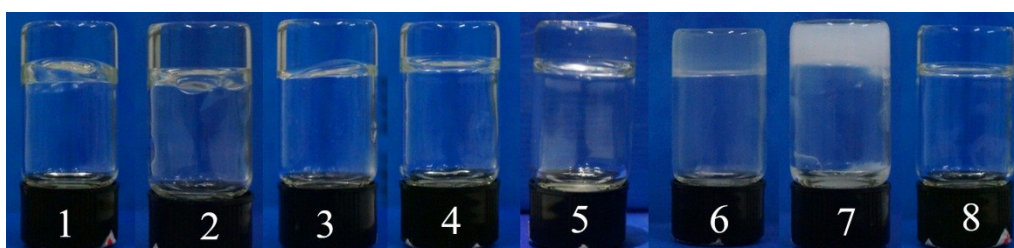


Figure S2. Photograph of POSS-Cys and POSS-Hpy gels in different solvents (25°C); 1, 2, 3 are POSS-Cys gel in benzene, styrene and carbon tetrachloride; 4, 5, 6, 7, 8 are POSS-Hpy gel in benzene, styrene, carbon tetrachloride, acetone and xylene.

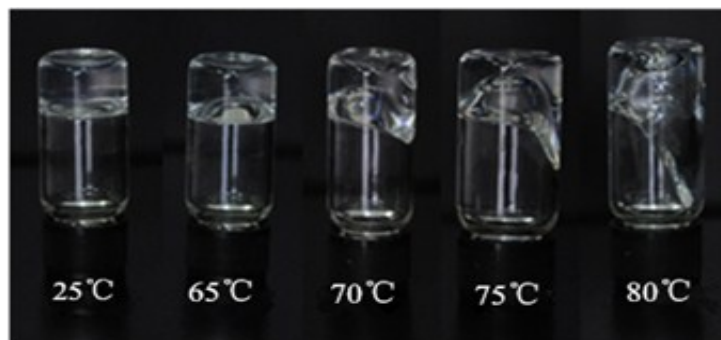


Figure S3. The dynamic changes of POSS-Cys gel in the process of gel being heated, 30 mg/mL in styrene.

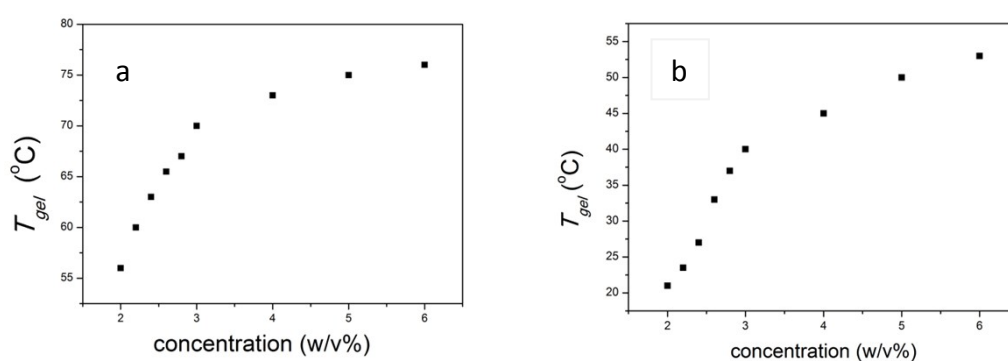


Figure S4. Phase diagram of POSS-Cys gels (a) and POSS-Hpy gels (b) in styrene.

Like the most traditional low molecular weight gels, as the concentration was increased, the T_{gel} values increased until a plateau region was reached, confirming the T_{gel} of POSS-Cys gel (75 °C) was 20 °C higher than the POSS-Hpy gel (55 °C), demonstrating the existence of sulfur improved the thermal stability of gels. In addition, a viscous flow state when the temperature increased to the T_{gel} point was observed, it seems likely that although it cannot hold itself in a solid-like state at the T_{gel} point, it keeps the viscoelasticity of the material to considerable extent just like the molten polymer (Figure S3). Generally, in low molecular weight gel systems, the sample-spanning gel networks were broken down to amounts of small aggregates which were dissolved in liquid phase at the T_{gel} point ⁶.

2.3 The morphology of POSS-Cys and POSS-Hpy xerogels

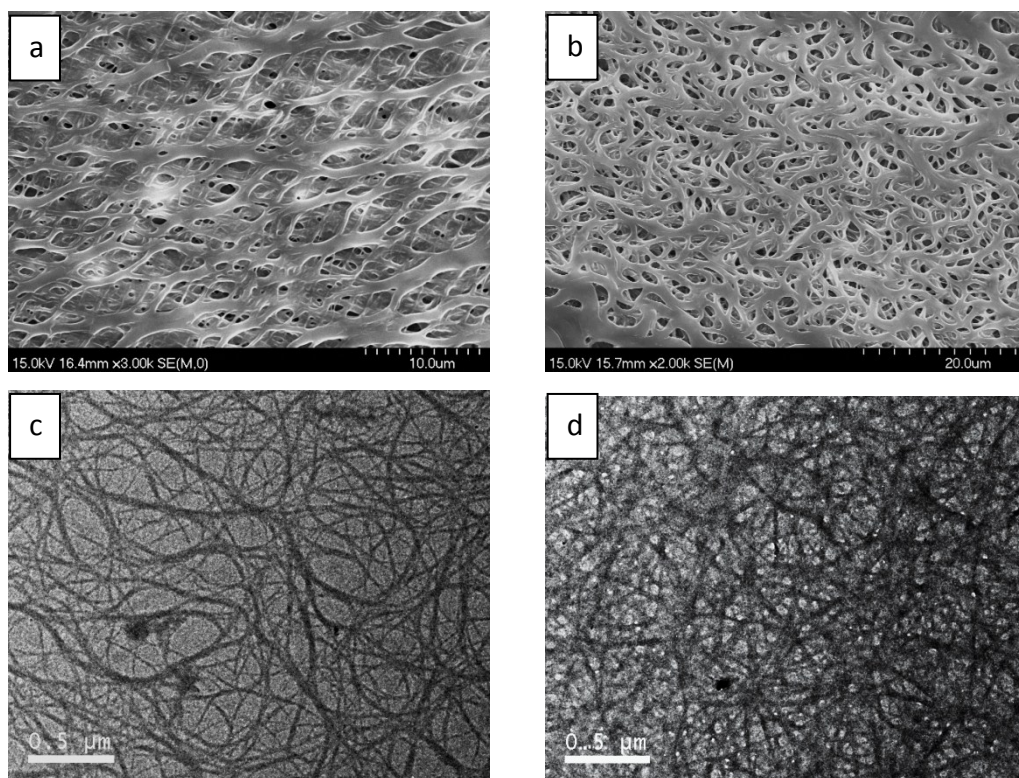


Figure S5. SEM and TEM images of POSS-Cys(a, c) and POSS-Hpy(b, d) xerogels.

The morphology of POSS-Cys and POSS-Hpy xerogels obtained from toluene were investigated by SEM and TEM, as shown in Figure S5. This demonstrated that as a result of the transformation of organic “arms” of the POSS dendrimer, the loofah-like three-dimensional (3D) gel networks could still be constructed. Particularly, in TEM, the relatively heavy Si atoms in the gelator allowed the assemblies formed by POSS-Cys and POSS-Hpy to be observed even in the absence of heavy atom staining agent, the gel fibre network had a 3D structure which performed a loofah-like network structure, in which all fibres connected to each other without start and end being observed. This endless and flexuous column orders themselves in a sectional type, formed a furcate and continuous structure. Interestingly, furcate fibres were once again obtained which induced irregular closed meshes. Importantly high-density junction points of the network were observed even at extremely low concentration, indicative of POSS-Cys and POSS-Hpy being born to undergo the “loofah-like” assembly model.

2.4 Rheological studies of gels

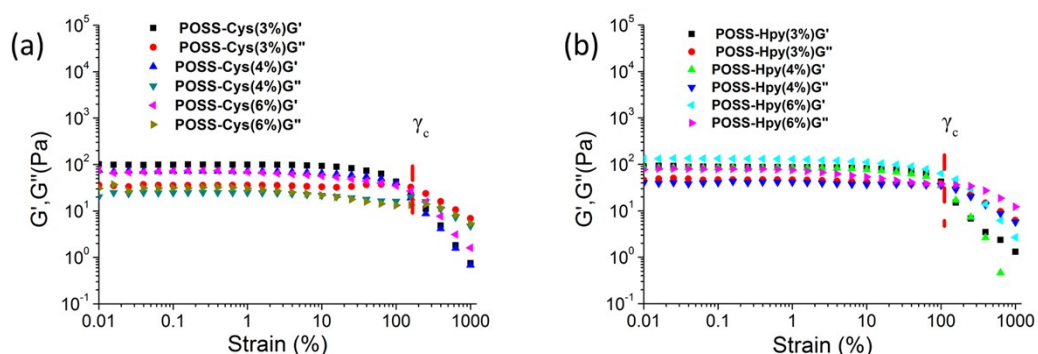


Figure S6. Strain dependence of G' and G'' for gels, measured at 25 °C with a strain from 0.01% to 1000% and frequency $\omega = 10 \text{ rads}^{-1}$; (a), (b) POSS-Cys and POSS-Hpy gels with different concentrations in styrene.

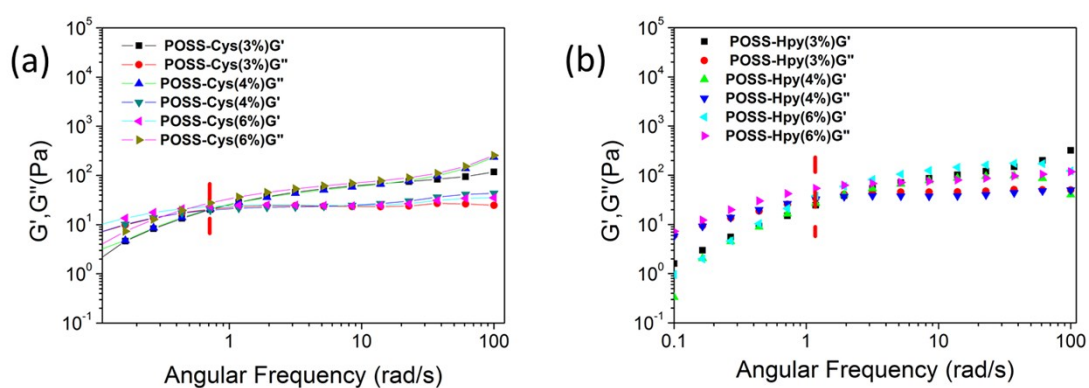


Figure S7. Frequency dependence of G' and G'' for gels, measured at 25 °C with a frequency from 0.01 to 100 rads^{-1} and strain $\gamma = 1\%$. (a), (b) POSS-Cys and POSS-Hpy gels with different concentrations in styrene.

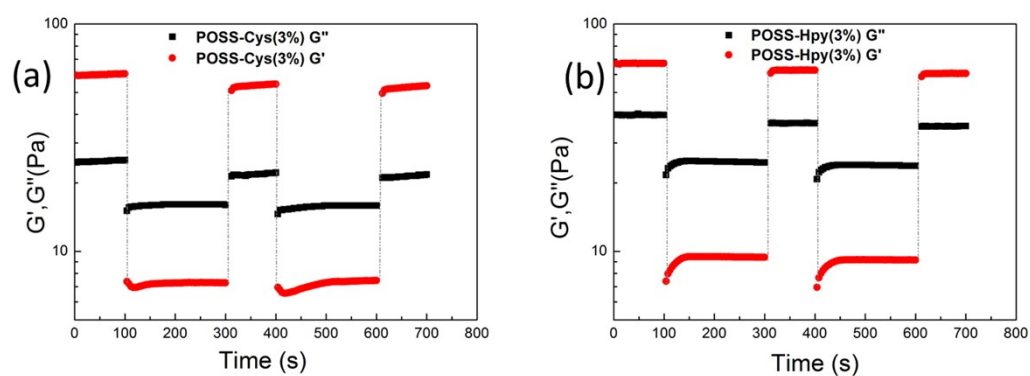


Figure S8. The G' and G'' dependence of time in continuous step strain measurements for gels; (a), (b) are recovery property of the gels and hybrid gels: the gel was first given a small strain

of 1% for 100 s and then subjected to a strong strain of 200% for 200 s, following small strain of 1% for its recovery. Then repeat twice to detect its reversibility, frequency keep in 6.28 rad s⁻¹.

Rheological measurements were carried out to investigate the mechanical properties and self-recovery properties of these gels. Dynamic strain sweep data showed the uppermost boundary of the linear viscoelastic region (LVR) about POSS-Cys and POSS-Hpy gels (Figure S6). The γ_c of POSS-Cys and POSS-Hpy gels are scarcely sensitive to the concentration of gelators. The increasing of gelator's concentration have no obvious influence on G' , G'' and γ_c , which means that a relatively stable gel network could be self-assemble in solvent at a quite low concentration of gelators with a strong ability to resistant the external stress⁷.

The G' (elasticity) and G'' (viscosity) as a function of ω for gels within linear deformation range were illustrated. From Figure S7, it can be clearly observed that the G' or G'' curves of POSS-Cys and POSS-Hpy gels essentially followed a similar trend, at low frequency where $G'' > G'$ ($\tan \delta > 1$), quasi-liquid behavior is dominating. As ω increased, there is a regional monotonic increase in moduli. Simultaneously, G' is gradually getting closer to G'' until a crossover point of G' and G'' curves appeared, suggesting the formation of an elastic gel network.⁸ After the crossover point where $G' = G''$, G' continued to increase to reach a plateau region and exceeded the G'' at high frequency range, whereas the curve of G'' reached its peak and kept it. The elastic character become the dominant factor at high frequency where $G' > G''$, the gels exhibited a typical solid-like character. These features corresponded to the typical viscoelastic material with a narrow distribution of relaxation time. The crossover point of POSS-Cys and POSS-Hpy gels are roughly estimated to be at the same $\omega \approx 0.8$ to 1.1 rad s⁻¹ where $G'(\omega) = G''(\omega) \approx 20$ and 70 Pa, which shows that the moduli curves of these kinds of gels are relatively independent of ω throughout the whole ω range, evidenced the formation of gel network structure.

POSS-Cys and POSS-Hpy gels exhibit very rapid recovery of its mechanical properties after a large-amplitude oscillatory break-down, known as thixotropic nature (Figure S7). Under the application of a large-amplitude oscillatory force (strain, $\gamma = 200\%$; frequency, $\omega = 6.28$ rad/s) the G' value decreased from 55 Pa to 5 Pa (POSS-Cys = 3 %) (Figure. S7a), resulted in a quasi-liquid state ($\tan \delta = 2.4$; $G''/G' < 3.0-4.0$). However, when the amplitude decreased ($\gamma = 0.1\%$) at the same frequency, G' recovered to its initial value immediately and the system returned to a quasi-

solid state ($\tan \delta = 0.4 < 0.4-0.5$). Using the same test method we investigated the POSS-Hpy gels, it also had the excellent recovery properties (Figure S7b).

2.5 Proposed mechanism of gelation

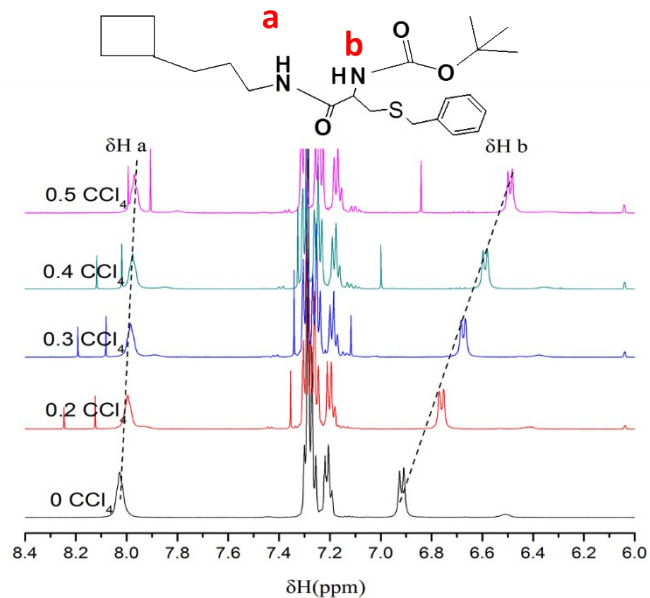


Figure S9. ^1H NMR spectra of POSS-Cys in DMSO- d_6 and with varying volume fraction of CCl_4 , the concentration of hybrid gelator is 0.5 % (2.5 mg, 0.5 mL).

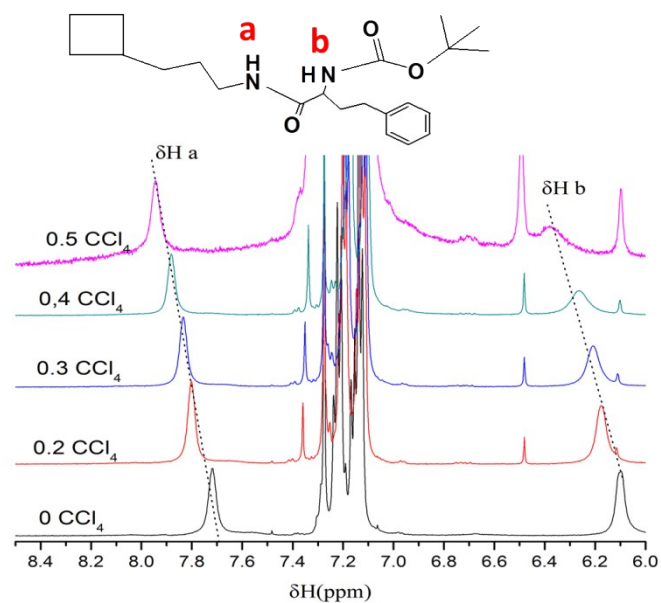


Figure S10. ^1H NMR spectra of POSS-Hpy in CDCl_3 and with varying volume fraction of CCl_4 , the concentration of hybrid gelator is 0.5 % (2.5 mg, 0.5 mL).

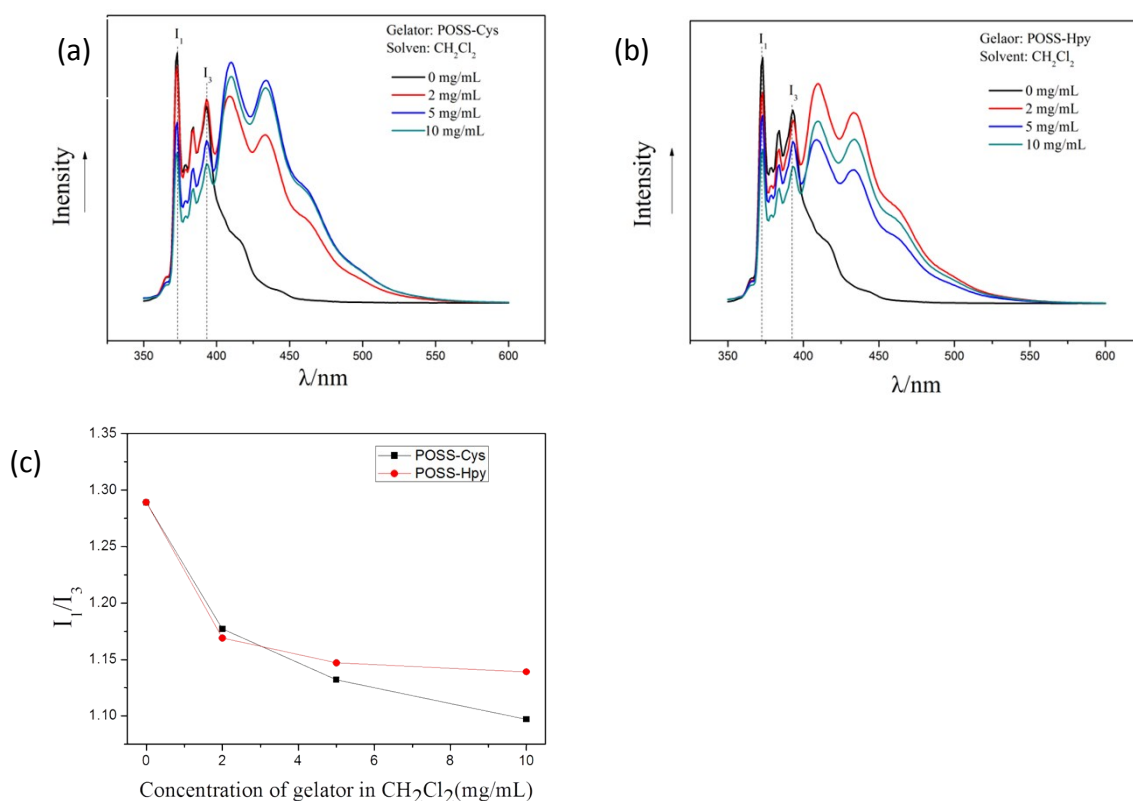


Figure S11. Fluorescence emission spectra of POSS-Cys (a) and POSS-Hpy (b) with pyrene (5 mg/mL) incorporated in CH₂Cl₂, excitation wavelength: 335 nm, temperature 25 °C; (c) I₁/I₃ ratio of gelators in CH₂Cl₂.

Figure S9 is the ¹H NMR spectra of POSS-Cys in DMSO-d₆ with varying volume fraction of CCl₄. It shows that the initially peaks of amide H (a), carbamate H (b) gradually got upfield shifted at higher varying volume fraction of CCl₄, which attributed to the weakening of hydrogen bonding interactions.⁹ This proved that the hydrogen bonding interaction involving amides and carbamate groups are the driving force for the gelation of POSS-Cys hybrid gelator.¹⁰ Figure S6 also proved that the hydrogen bonding interaction involving amides and carbamate is the driving force for the gelation of POSS-Hpy hybrid gelator.

Studies on the polarity of the interior of the aggregate are carried out by using the fluorescence emission of pyrene in the gel state.¹¹ The I₁ peak, which arise from the 0-0 transition from the lowest state excited electronic state to the lowest ground state, is a symmetry-forbidden transition that can be enhanced by distortion of the π-electron cloud. On the other the I₃ peak is relatively solvent insensitive because it is not a forbidden transition. Consequently, the I₁/I₃ is a measure of the polarity of the environment. The observed I₁/I₃ of POSS-Cys ranges from about

1.28 in low concentration of gelators to about 1.0 in in low concentration of gelators. The changes in I_1/I_3 value demonstrated the formation of π - π stacking.¹² What's more I_1/I_3 of POSS-Hpy changes in I_1/I_3 value also demonstrated the formation of π - π stacking.

Reference:

- 1 G. Tang, S. Chen, F. Ye and Xu. Wang, *Chem. Commun.*, 2014, **50**, 7180.
- 2 M. Brust, M. Walker, D. J. Bethell. *Chem. Soc., Chem. Commun.*, 1994, **7**, 801.
- 3 K. Kalyanasundaram, J. K. Thomas, *J. Am. Chem. Soc.* 1977, **99**, 2039.
- 4 W. Edwards, C. A. Lagadec, D. K. Smith, *Soft Matter*, 2011, **7**, 110.
- 5 M. Takeuchi, S. Kageyama, H. Suzuki, *Colloid. Polym. Sci.*, 2003, **281**, 1178.
- 6 A. R. Hirst, D. K. Smith, M. C. Feiters and H. P. M. Geurts, *Langmuir*, 2004, **20**, 7070.
- 7 A. R. Hirst, I. A. Coates, T. R. Boucheteau, *J. Am. Chem. Soc.*, 2008, **130**, 9113.
- 8 Y. Wang, L. Chen, *Carbohydr. Polym.*, 2011, **83**, 1937.
- 9 Y. Ebara, K. Itakura, Y. Okahata, *Langmuir*, 1996, **12**, 5165.
- 10 A. Ajayaghosh, S. J. George, *J. Am. Chem. Soc.* 2001, **123**, 5148.
- 11 S. Ganesh, S. Prakash, R. Jayakumar, *Biopolymers*, 2003, **70**, 346.
- 12 J. Rubio, I. Alfonso, M. I. Burguete, S. V. Luis, *Soft Matter*, 2011, **7**, 10737.